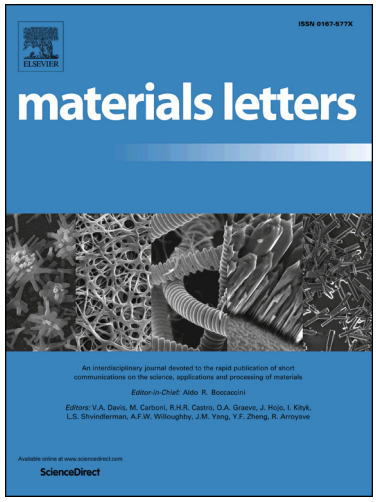

Electrochemical assessment of $Ca_3Co_4O_9$ nanofibres obtained by Solution Blow Spinning

Vinícius D. Silva, Thiago A. Simões, Francisco J.A. Loureiro, Duncan P. Fagg, Eliton S. Medeiros, Daniel A. Macedo

PII: S0167-577X(18)30452-X
DOI: https://doi.org/10.1016/j.matlet.2018.03.088
Reference: MLBLUE 24049

To appear in: *Materials Letters*

Received Date: 14 January 2018
Revised Date: 17 March 2018
Accepted Date: 17 March 2018

Please cite this article as: V.D. Silva, T.A. Simões, F.J.A. Loureiro, D.P. Fagg, E.S. Medeiros, D.A. Macedo, Electrochemical assessment of $Ca_3Co_4O_9$ nanofibres obtained by Solution Blow Spinning, *Materials Letters* (2018), doi: https://doi.org/10.1016/j.matlet.2018.03.088

Electrochemical assessment of $Ca_3Co_4O_9$ nanofibres obtained by Solution Blow Spinning

Vinícius D. Silva[a,b], Thiago A. Simões[a], Francisco J. A. Loureiro[c], Duncan P. Fagg[c]

Eliton S. Medeiros[a,b], Daniel A. Macedo[a,*]

[a] Materials Science and Engineering Postgraduate Program, UFPB, 58051-900, João Pessoa, Brazil

[b] Materials and Biosystems Laboratory (LAMAB), DEMAT, UFPB, 58051-900, João Pessoa, Brazil

[c] Department of Mechanical Engineering, University of Aveiro, 3810-193 Aveiro, Portugal

Abstract

$Ca_3Co_4O_9$ (C349) nanofibres were obtained by Solution Blow Spinning (SBS) and evaluated as electrocatalysts for Oxygen Reduction and Oxygen Evolution Reactions (ORR and OER). Calcined nanofibres were characterised in terms of structural, morphological and electrochemical features. Results showed that catalytic activity of C349 nanofibres for ORR/OER is in line with literature data for carbon-related materials. The areal capacitance is much better than that of TiO_2 nanotubes.

Keywords: Solution blow spinning; fibre technology; energy storage and conversion.

*Corresponding author. Tel.: +55 83 32167860; fax: +55 83 32167906.

E-mail address: damaced@gmail.com (Daniel A. Macedo)

1. Introduction

Climate change has summoned the attention of the world population due to the impact of polluting agents. Since this pollution brings severe economic and environmental impacts there is an urgent need for the improvement of current energy conversion/storage technologies to bring about a drastic reduction in our dependence on fossil fuels [1]. In this sense, ORR and OER play a vital role

in the performance of eco-friendly energy conversion and storage devices [2]. Platinum is among the best catalysts for these electrochemical reactions [3]. However, due to its high cost, efforts have been made to develop metal oxide catalysts that can combine improved electrochemical activity with low cost [4]. Moreover, calcium-cobaltites (such as $Ca_3Co_4O_9$, hereafter called C349) have been widely investigated for energy-related applications [5-7]. The electrochemical performance of powdered C349 as a potential electrode for ORR/OER has already been reported [8]. However, there is no report on the electrochemical activity of C349 fibres. Ceramic fibres have attracted substantial attention because of their large aspect ratio and unique properties that may enhance the kinetics of the electrochemical reactions [9].

In this work, C349 nanofibres were prepared by SBS, which has emerged as a simple, fast and cost-effective technique that can rival electrospinning as a scalable route to obtaining micron and nanofibrous materials [9–11]. Electrochemical properties of calcined fibres were evaluated aiming to attain potential electrodes for energy-related applications.

2. Experimental

0.9 g of Polyvinylpyrrolidone (PVP, Mw = 1,300,000 g/mol) was dissolved in 10 mL of ethanol. Then, stoichiometric amounts of calcium ($Ca(NO_3)_2{\cdot}4H_2O$, Merck) and cobalt ($Co(NO_3)_2{\cdot}6H_2O$, Merck) nitrates were dissolved in 5 mL of methanol under constant stirring. Afterwards, the nitrate solution (rose-red colour) was slowly added to the PVP solution and stirred for a few hours to form the precursor solution used in the SBS system. A composite mat (nitrates/polymer) was obtained onto an aluminium foil wrapped on the collector that had been preheated at 60 °C. Fibres were produced using the following experimental parameters: pressure of 0.41 MPa, injection rate of 2.5 mL/h and working distance of 60 cm. The spun mat was kept at 60 °C for 12 h for complete solvent removal and then calcined at 850 °C for 2 h in air at a heating rate of 2 °C/min. Calcined fibres were characterised by X-ray diffraction (XRD, D2PHASER, BRUKER)

using Cu-Kα radiation (λ = 1.5418 Å). FTIR spectra of the as-spun and calcined fibres were obtained by using a Shimadzu IRAffinity-1 spectrometer. Fibre morphology and energy dispersive spectroscopy (EDS) analysis were assessed using a field-emission gun scanning electron microscopy (FESEM, Carl Zeiss, Supra 35-VP Model). The chemical states at the fibre surface were further studied using X-ray photoelectron spectroscopy (XPS). Details on the XPS analysis can be found in Electronic Supporting Information (ESI). Cyclic voltammetry (CV), linear sweep voltammetry (LSV) and electrochemical impedance spectroscopy (EIS) were used to assess the performance of the C349 electrode using Autolab PGSTAT101 (for CV and LSV) and PGSTAT302N (for EIS in the frequency range 100 kHz to 0.01 Hz). Platinum and Ag/AgCl were used as counter and reference electrodes, respectively. C349 fibres and glassy carbon (GC, 3 mm diameter) were used as working electrodes. Details on the preparation of C349 working electrodes can be found in a previous work [8], as well as in ESI.

3. Results and Discussion

The XRD pattern of calcined fibres, Fig. 1a, was able to be indexed using ICSD 151436 and 95439 cards, characterising a monoclinic-type structure consisting of $Ca_2CoO_{3-\delta}$ and CoO_2 subsystems, as expected for misfit-layered Ca-cobaltites. Morphological characterisation of the calcined fibres (Fig. 1b and 1c) shows interconnected nanoplatelets with irregular shape and average diameter of 324 nm. This structure is similar to that reported for C349 electrospun fibres [12]. EDS mapping (Fig. 1d) shows a uniform distribution of Ca, Co and O elements. FT-IR spectra, shown in Fig. S1, confirm the presence of amines group of PVP (band at 1290 cm^{-1}) and metal-oxygen bonds (Ca-O and Co-O) in the as-spun and calcined fibres, respectively. The XPS spectra of C349 (Fig. 1e) showed binding energy regions of Co 2p, O 1s, C 1s and Ca 2p. Fig. 1f depicts the core level of high resolution

spectra of the Co $2p_{3/2}$ region, deconvoluted to reveal the cobalt oxidation states Co^{2+} (43 %), Co^{3+} (34 %) and Co^{4+} (22.1 %) in agreement with literature values [13,14].

Figure 1.

Fig. 2a compares the performance of bare GC and C349 electrodes for the ORR. C349 showed activity to ORR around -0.70 V with current peak of 18.74 μA, which is higher than the current value reported for $Ca_3Co_4O_9$-monocrystals [8]. In addition, GC presented a lower activity to ORR, around -0.68 V with peak current of 9.06 μA. The OER activity of the C349 was evaluated by LSV in a potential range from 0.1 to 1.7 V in 0.1 M KOH (Fig. 2b). Pt-wire was used for comparative purposes. C349 again showed superior catalytic activity to OER compared to GC. At 5 mA/cm², C349 presented a potential of 0.89 V against 1.48 V for GC, similar to that found for other OER catalysts listed in Table 1. The mixed Co^{4+}/Co^{3+} redox couple highlighted by the XPS could be the likely source of the noted catalysis of the OER [14]. Pt-wire (measuring 0.63 V) was better than C349 and CG for the OER, as expected.

Figure 2.

Table 1.

Fig. 3a shows that CV curve has a non-rectangular pattern, evidencing a charge storage mechanism governed by Faradic processes [15]. It suggests that C349 has a pseudo-capacitive behaviour. The direct relation (Fig. 3b) between the scan rate (v) and voltammetric current (i) was performed and the best fit was obtained for $i \propto \sqrt{v}$, suggesting a capacitance dominated by a bulk diffusion process [16]. Fig. 3c shows the capacitance as a function of the scan rate. The capacitance decreases with increasing scan-rate, as a result of the ion-exchange mechanism process, where low scan-rates favour the intercalation of ions throughout the electrode structure, otherwise the ion intercalation process ends up being limited [17]. The highest areal capacitance of 24.8 mF/cm^2 at 10 mV/s is 1240 times higher than that of TiO_2 nanotubes (0.02 mF/cm^2) [22]. This could be attributed to a reversible electron transfer process of the Co^{4+}/Co^{3+} redox couple. Fig. 3d depicts the Nyquist

plot (acquired in 1 M KOH) of the C349 electrode. The high frequency intercept at the real axis indicates a resistance of the electrochemical system of ~ 23 Ω. The almost vertical line at low frequencies confirms the pseudo-capacitive behaviour of the C349. Moreover, the absence of a high frequency semicircle may be ascribed to the fast charge-transfer speed during the Faradaic reactions [23,24].

Figure 3.

4. Conclusion

$Ca_3Co_4O_9$ nanofibres were successfully obtained by SBS. The electrochemical assessment of the electrode derived from solution blow spun nanofibres showed promising performance for ORR and OER. The results exceed the performance of carbon related materials and are also better than those of TiO_2 nanotubes from literature.

Acknowledgements

The authors acknowledge CNPq (311883/2016-8) and FCT, project grant PTDC CTM-ENE/6319/2014, the FCT Investigator Programme, project IF/01344/2014/CP1222/CT0001, QREN, FEDER and COMPETE Portugal and the European Union.

References

[1] S. Chu, A. Majumdar, Nature 488 (2012) 294–303.

[2] J. Lee, B. Jeong, J.D. Ocon, Curr. Appl. Phys. 13 (2016) 309–321.

[3] A. Serov, N.I. Andersen, A.J. Roy, I. Matanovic, K. Artyushkova, P. Atanassov, J. Electrochem. Soc. 162 (2015) F449–F454.

[4] Q. Zhao, Z. Yan, C. Chen, J. Chen, Chem. Rev. 117 (2017) 10121–10211.

[5] M.A. Madre, F.M. Costa, N.M. Ferreira, A. Sotelo, M.A. Torres, G. Constantinescu, S. Rasekh, J.C. Diez, J. Eur. Ceram. Soc. 33 (2013) 1747–1754.

[6] C.G.M. Lima, R.M. Silva, F. de M. Aquino, B. Raveau, V. Caignaert, M.R. Cesário, D.A. Macedo, Mater. Chem. Phys. 187 (2017) 177–182.

[7] G.G. Yadav, A. David, T. Favaloro, H. Yang, A. Shakouri, J. Caruthers, Y. Wu, J. Mater. Chem. A 1 (2013) 11901–11908.

[8] C.S. Lim, C.K. Chua, Z. Sofer, O. Jankovsky, M. Pumera, Chem. Mater. 26 (2014) 4130−4136.

[9] S. Peng, L. Li, J. Kong Yoong Lee, L. Tian, M. Srinivasan, S. Adams, S. Ramakrishna, Nano Energy 22 (2016) 361–395.

[10] J. V. Patil, S.S. Mali, A.S. Kamble, C.K. Hong, J.H. Kim, P.S. Patil, Appl. Surf. Sci. 423 (2017) 641–674.

[11] E.S. Medeiros, G.M. Glenn, A.P. Klamczynski, W.J. Orts, L.H.C. Mattoso, J. Appl. Polym. Sci. 113 (2009) 2322–2330.

[12] K.A. Sekak, A. Lowe, J. Am. Ceram. Soc. 94 (2011) 611–619.

[13] Y. Huang, B. Zhao, R. Ang, S. Lin, Z. Huang, S. Tan, Y. Liu, W. Song, Y. Sun, J. Phys. Chem. C 117 (2013) 11459–11470.

[14] S. Yu, S. He, H. Chen, L. Guo, J. Power Sources 280 (2015) 581–587.

[15] S. Zhang, N. Pan, Adv. Energy Mater. 5 (2015) 1–19.

[16] B. Vidhyadharan, N.K.M. Zain, I.I. Misnon, R.A. Aziz, J. Ismail, M.M. Yusoff, R. Jose, J. Alloys Compd. 610 (2014) 143–150.

[17] S. Vijayakumar, S.H. Lee, K.S. Ryu, Electrochim. Acta 182 (2015) 979–986.

[18] C. Sun, F. Li, C. Ma, Y. Wang, Y. Ren, W. Yang, Z. Ma, J. Li, Y. Chen, Y. Kim, L. Chen, J. Mater. Chem. A 2 (2014) 7188–7196.

[19] Q. Wang, X. Qiu, W. Hu, Y. Huang, Mater. Lett. 190 (2017) 169–172.

[20] W.G. Hardin, D.A. Slanac, X. Wang, S. Dai, K.P. Johnston, K.J. Stevenson, J. Phys. Chem. Lett. 4 (2013) 1254–1259.

[21] C. Si, Y. Zhang, C. Zhang, H. Gao, W. Ma, L. Lv, Z. Zhang, Electrochim. Acta 245 (2017) 829–838.

[22] Z. Li, Y. Ding, W. Kang, C. Li, D. Lin, X. Wang, Z. Chen, M. Wu, D. Pan, Electrochim. Acta 161 (2015) 40–47.

[23] J. Wang, W. Dou, X. Zhang, W. Han, X. Mu, Y. Zhang, X. Zhao, Y. Chen, Z. Yang, Q. Su, E. Xie, W. Lan, X. Wang, Electrochim. Acta 224 (2017) 260-268.

[24] X. Ji, S. Cheng, L. Yang, Y. Jiang, Z. Jiang, C. Yang, H. Zhang, M. Liu, Nano Energy 11 (2015) 736-745.

Table 1 - Literature survey on electrochemical performance of metal oxide catalysts towards OER.

Catalyst	Electrolyte	OER potential (V) at 5 mA/cm^2	Reference
Graphene-Co_3O_4	0.1 M KOH	0.73 vs. SCE	[18]
Co_3O_4/N-doped carbon	0.1 M KOH @ 1600 rpm	0.93 vs. Ag/AgCl at 10 mA/cm²	[19]
$LaNiO_3$/N-doped carbon	0.1 M KOH	1.62 vs RHE	[20]
$CoFe_2O_4$, $NiFe_2O_4$ and $MnFe_2O_4$	0.1 M KOH @ 1600 rpm	1.57 V, 1.57 V and 1.65 V vs. RHE at 10 mA/cm²	[21]
$Ca_3Co_4O_9$ nanofibres	0.1 M KOH	0.89 vs Ag/AgCl	This work

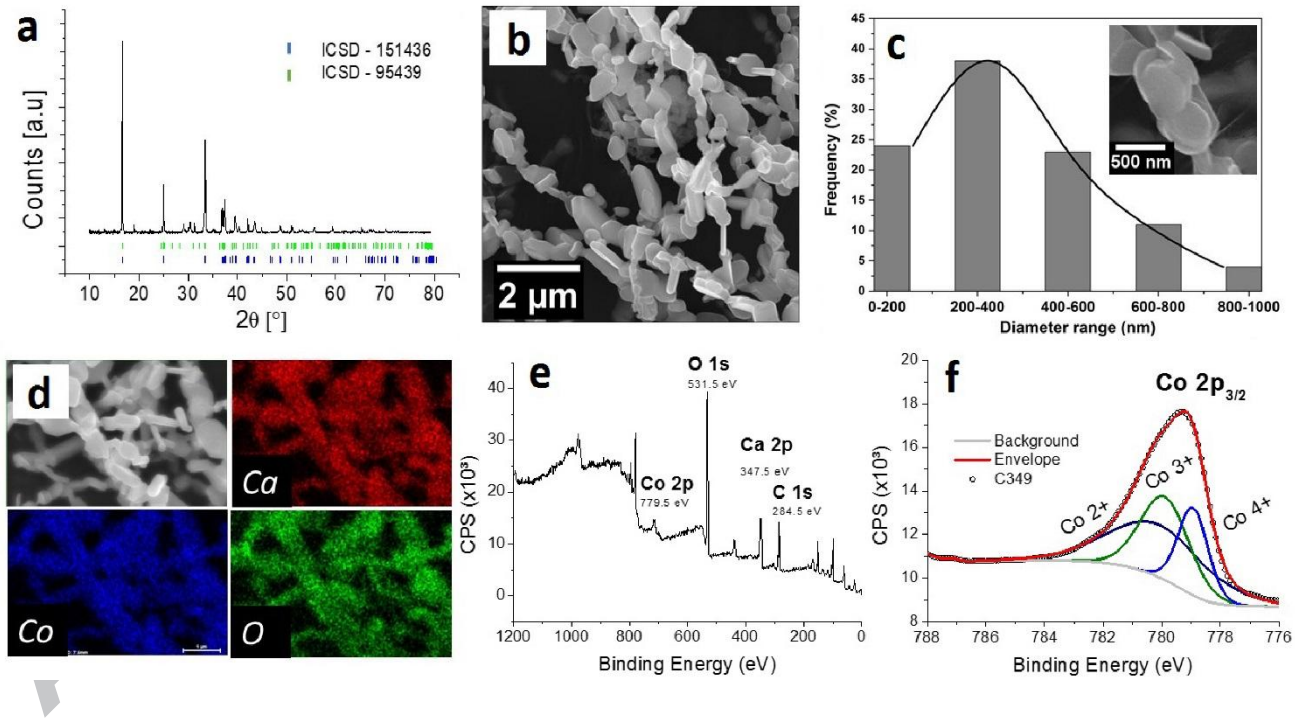

Fig. 1 – (a) XRD pattern, (b) FESEM image, (c) diameter distribution, (d) EDS mapping, (e) and (f) XPS spectra.

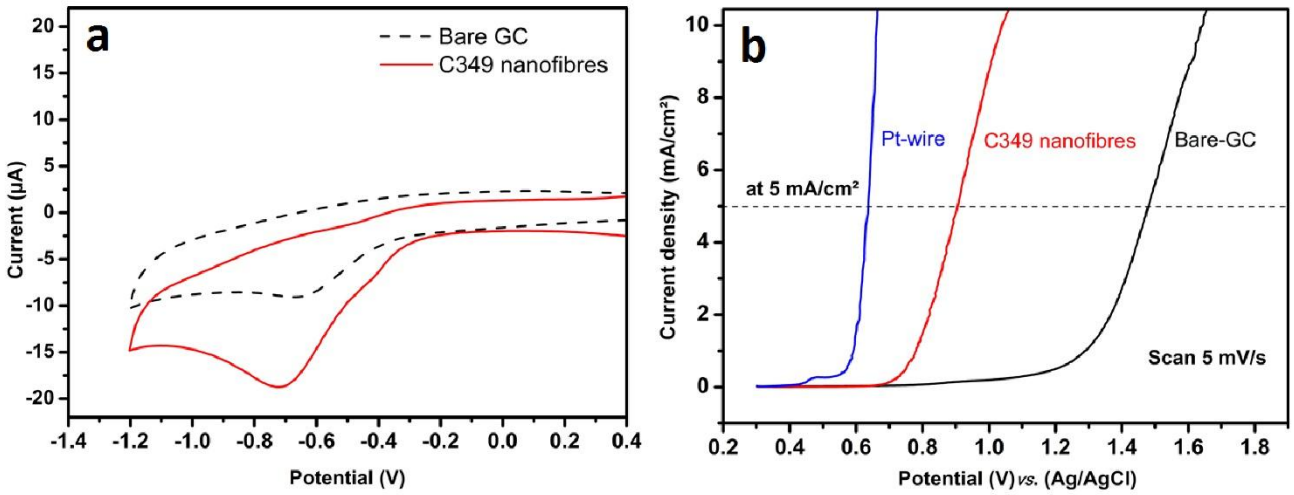

Fig. 2 – (a) CV of C349 and bare GC in 10 mM potassium hydroxide and scan rate of 100 mV/s; (b) LSV of Pt-wire, C349 and GC in 0.1 M KOH.

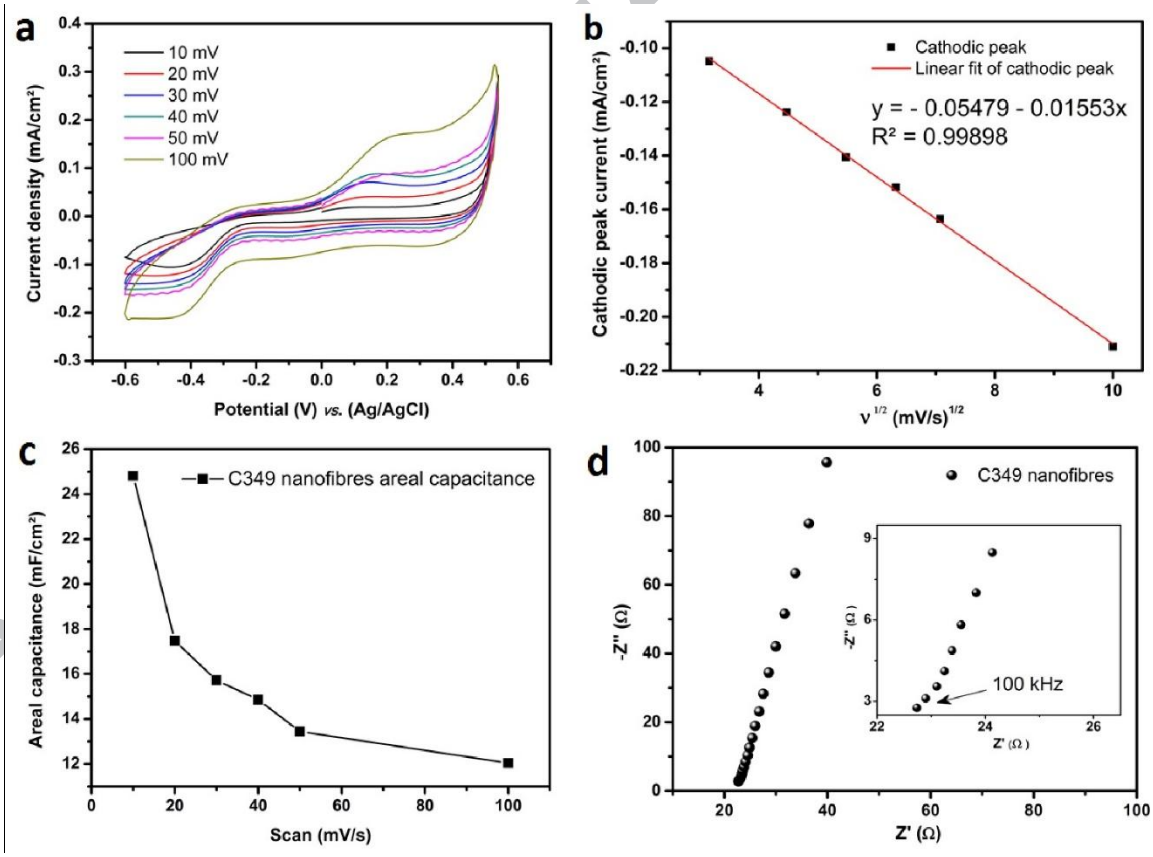

Fig. 3 – (a) CV curves of C349 in 1 M KOH, (b) square root variation of the cathodic peak current with scan rate, (c) areal capacitance as a function of the scan rate, and (d) Nyquist plot.

Highlights

- $Ca_3Co_4O_9$ nanofibres synthesized by Solution Blow Spinning;
- $Ca_3Co_4O_9$ nanofibres as electrocatalysts for oxygen reduction and oxygen evolution reactions;
- Areal capacitance at 10 mV/s is 1240 times higher than that of TiO_2 nanotubes.